Comparative Studies of the Properties of Poly(methyl methacrylate)–Clay Nanocomposite Materials Prepared by *In Situ* Emulsion Polymerization and Solution Dispersion

Jui-Ming Yeh,[1] Shir-Joe Liou,[1] Mei-Chun Lai,[1] Yu-Wen Chang,[1] Cheng-Yu Huang,[1] Chen-Ping Chen,[1] Jenn-Huey Jaw,[1] Tsung-Yen Tsai,[1] Yuan-Hsiang Yu[2]

[1]*Department of Chemistry and Center for Nanotechnology, Chung-Yuan Christian University, Chung Li, Taiwan 32023, Republic of China*
[2]*Department of Electronic Engineering, Lan-Yan Institute of Technology, I-Lan 261, Taiwan, Republic of China*

Received 4 March 2004; accepted 4 June 2004
DOI 10.1002/app.21095
Published online in Wiley InterScience (www.interscience.wiley.com).

ABSTRACT: A series of polymer–clay nanocomposite (PCN) materials consisting of organic poly(methyl methacrylate) (PMMA) and inorganic montmorillonite (MMT) clay platelets were prepared successfully by the effective dispersion of nanolayers of the MMT clay in the PMMA framework through both *in situ* emulsion polymerization and solution dispersion. The as-prepared PCN materials obtained with both approaches were subsequently characterized with wide-angle powder X-ray diffraction and transmission electron microscopy. For a comparison of the anticorrosion performance, a PCN material (e.g., 3 wt % clay loading) prepared by *in situ* emulsion polymerization, showing better dispersion of the clay platelets in the polymer matrix, exhibited better corrosion protection in the form of a coating on a cold-rolled steel coupon than that prepared by solution dispersion, which showed a poor dispersion of the clay nanolayers according to a series of electrochemical corrosion measurements. Comparative studies of the optical clarity, molecular barrier properties, and thermal stability of samples prepared in both ways, as membranes and fine powders, were also performed with ultraviolet–visible transmission spectroscopy, molecular permeability analysis, thermogravimetric analysis, and differential scanning calorimetry. © 2004 Wiley Periodicals, Inc. J Appl Polym Sci 94: 1936–1946, 2004

Key words: nanocomposites; clay; corrosion

INTRODUCTION

Nanocomposite materials have drawn great attention because of their unique physical and chemical properties, which are dramatically different from those of conventional microcomposites.[1–3] Polymer–clay nanocomposite (PCN) materials exhibit increased modulus,[4–9] decreased thermal expansion coefficients,[5] reduced gas permeability,[5,10] increased solvent resistance,[11] enhanced ionic conductivity,[12] and corrosion protection[8,9,13–17] in comparison with the bulk polymers. The early historical development of PCN can be traced back to research on polyamide–clay nanocomposites reported by Toyota's group in 1990.[18]

Poly(methyl methacrylate) (PMMA) belongs to the family of polyacrylic and methacrylic esters and possesses many desirable properties (e.g., exceptional optical clarity, good weatherability, high strength, and excellent dimensional stability). According to previously published studies,[19–25] PMMA–clay nanocomposites have potential applications for reduced gas permeability, improved physical performance, and increased heat resistance, without any sacrifice in optical clarity.[19–25] Recently, we have found that the incorporation of nanolayers of montmorillonite (MMT) clay into a polymer framework (e.g., PMMA) via *in situ* solution polymerization can effectively enhance the corrosion protection of bulk polymeric coatings on cold-rolled steel (CRS) coupons.[14] In that study, the weight-average molecular weight (M_w) of PMMA prepared by *in situ* solution polymerization was approximately 39,000, and a poor dispersion of clay platelets existed in the polymer framework. According to many published articles,[27,28] PCN materials prepared by *in situ* emulsion polymerization have the following characteristics: PMMA has a much higher value of M_w, and a better dispersion of clay nanolayers exists in the polymer framework. However, a comparative study of the various properties of PCN materials prepared with different dispersion capabilities of the clay platelets in the polymer framework has never been reported.

Therefore, in this article, we compare the properties of PMMA–clay nanocomposite materials prepared by

Correspondence to: J.-M. Yeh (juiming@cycu.edu.tw).
Contract grant sponsor: National Science Council; contract grant number: 92-2113-M-033-011.

in situ polymerization (i.e., better dispersion of clay platelets) and solution dispersion (i.e., poor dispersion of clay nanolayers). For example, we synthesized PMMA–clay with a 3 wt % clay loading (ECMA3). The M_w value of PMMA extracted from ECMA3 was found to be 351,100. For reasonable comparative studies, commercial PMMA (M_w = 350,000) was chosen for the preparation of PMMA–clay nanocomposite materials with a 3 wt % clay loading (SCMA3). Comparative studies on the corrosion protection, optical clarity, molecular barrier properties, and thermal stability of ECMA3 and SCMA3, as coatings, membranes, and fine powders, were also conducted with electrochemical corrosion measurements, ultraviolet–visible (UV–vis) transmission spectroscopy, gas permeability analysis (GPA), thermogravimetric analysis (TGA), and differential scanning calorimetry (DSC).

EXPERIMENTAL

Chemicals and instrumentation

Benzoyl peroxide (BPO; Riedel-de Haën; 98%, Seelze, Germany), 1-methyl-pyrrolidinone (NMP; Tedia; 99.6% Ohio, USA), hydrochloric acid (Riedel-de Haën; 37% Seelze, Germany), diethyl ether (Aldrich; 99% Ohio, USA), and commercial PMMA (Acros; M_w = 350,000) were used as received without further purification. Methyl methacrylate (MMA: Riedel-de Haën; 99% Seelze, Germany) was distilled under reduced pressure. [2-(Dimethylamino)ethyl]triphenylphosphonium bromide (Aldrich; 97% Wisconsin, USA) was used as an intercalating agent. Dimethyl dihexadecyl ammonium chloride (Hoclean; 75% Berlin, Germany) was used as a surfactant during the processing of *in situ* emulsion polymerization. The MMT clay, purchased from Pai-Kong Ceramic Co. (Taiwan), had a cationic exchange capacity value of 95 mequiv/100 g and the unit cell formula $Na^{+}_{0.31}[Al_{1.67}Mg_{0.33}]Si_4O_{10}(OH)_2 \cdot 5.8H_2O$.

A wide-angle X-ray diffraction (XRD) study of the samples was performed on a Rigaku D/MAX-3C OD-2988N X-ray diffractometer with a copper target and a nickel filter at a scanning rate of 2°/min. The samples for transmission electron microscopy (TEM) were first prepared by the powder of PCN materials being placed into PMMA resin capsules, and this was followed by the curing of the PMMA resin at 100°C for 24 h in a vacuum oven. The cured PMMA resin containing PCN materials was microtomed with a Reichert-Jung Ultracut-E into 60–90-nm-thick slices. Subsequently, one layer of carbon about 10 nm thick was deposited on these slices on 100-mesh copper nets for TEM observations on a JEOL 200FX with an acceleration voltage of 120 kV. The electrochemical measurements of the corrosion potential [E_{corr} (V)], polarization resistance [R_p (Ω/cm^2)], corrosion current (i_{corr}), and impedance spectroscopy on sample-coated CRS coupons were performed on a VoltaLab model 21 or 40 potentiostat/galvanostat in a standard corrosion cell equipped with two graphite-rod counter electrodes and a saturated calomel electrode (SCE) as well as a working electrode. A gas permeability analyzer (GTR 10, Yanagimoto Co., Ltd.) was used to perform the permeation experiments with oxygen gas. The permeation of water vapor was determined with an apparatus employed in our previously published studies.[7–9] The molecular weights of the polymers extracted from all the composite samples as well as bulk PMMA were determined on a PerkinElmer model TC4 equipped with a model 590 programmable solvent-delivery module, a differential refractometer detector, and a Styragel HT column with tetrahydrofuran (THF) as the eluant and monodispersed polystyrenes as calibration standards. UV–vis transmission spectra were obtained with a Hitachi U-2000 UV–vis spectrometer. A PerkinElmer thermal analysis system equipped with a model 7 DSC instrument and a model 7/DX TGA instrument was employed for the thermal analyses under air flow. The programmed heating rate was 20°C/min.

Preparation of the organophilic clay

The organophilic clay was prepared by a cation-exchange reaction between the sodium cations of the MMT clay and the quaternary alkylphosphonium cations [$P^{+}(Ph)_3CH_2CH_2CH_2N(CH_3)_2$] of the intercalating agent. The following equation was used to calculate the intercalating agent used for the cation-exchange reaction:

$$95/100 \times 5 \text{ g (for clay)} \times 1.2 = (X/M_w \text{ of intercalating agent}) \times 1 \times 1000$$

where X represents the amount of the intercalating agent, 95/100 represents the CEC value per 100 g of MMT clay, and 1.2 (>1) indicates that an excess amount of the intercalating agent was used. Typically, 5 g of MMT clay with a CEC value of 95 mequiv/100 g was stirred in 400 mL of distilled water (beaker A) at room temperature overnight. A separate solution contained an excess of the intercalating agent (2.36 g) in another 30 mL of distilled water (beaker B) under magnetic stirring, and this was followed by the addition of a 1*M* HCl aqueous solution to adjust the pH value to about 3–4. After 1 h of stirring, the solution containing the intercalating agent (beaker B) was added at a rate of approximately 10 mL/min with vigorous stirring to the MMT suspension (beaker A). The mixture was stirred overnight at room temperature. The organophilic clay was recovered by ultracentrifugation (at 9000 rpm for 30 min) and filtration of the solution in a Buchner funnel. The purification of

the raw products was performed through the washing and filtering of the samples, repeated at least three times, to remove excessive phosphonium ions.

Preparation of PMMA by emulsion polymerization

The typical procedure for the preparation of PMMA through conventional emulsion polymerization was as follows. Dimethyl dihexadecyl ammonium chloride (0.30 g; a surfactant) dissolving in 100 mL of distilled water was kept under magnetic stirring for 2 h. Nitrogen gas was bubbled into the flask throughout the reaction. MMA (22.44 g) was subsequently added to the solution, and the solution was stirred for an additional 3 h. BPO (2.48 g) was placed in a 250-mL, three-necked, round-bottom flask connected to a condenser, a thermometer, and a nitrogen gas inlet and outlet. Under magnetic stirring, the solution was heated to 85°C and kept there for 24 h. After the reaction was complete, 10 mL of diethyl ether was added to the mixing solution, and the solution was stirred for 30 min. Then, the as-prepared solution was poured into about 300 mL of distilled water to precipitate the polymer. After filtration, the purified polymer was dried *in vacuo* at room temperature for 48 h. PMMA (20.00 g) was obtained in an approximately 90% yield.

Preparation of the PMMA–clay nanocomposite materials by *in situ* emulsion polymerization

In a typical procedure for the preparation of PCN materials with a 1 wt % clay loading, first an appropriate amount of the organophilic clay (0.1 g) was added to 100 mL of distilled water under magnetic stirring overnight at room temperature. Dimethyl dihexadecyl ammonium chloride (0.30 g) was added, and the mixture was stirred for 2 h. MMA (9.90 g) was subsequently added to the solution, which was stirred for another 24 h, and nitrogen gas was bubbled into the flask throughout the reaction. Upon the addition of BPO (0.224 g), the solution was stirred for 24 h at 85°C under an atmosphere of N_2. After the reaction was completed, 10 mL of diethyl ether was added to the mixing solution, and the solution was stirred for 30 min. The as-synthesized emulsion solution was subsequently added to 300 mL of distilled water, and the resultant product was obtained by filtration and subsequent drying under a dynamic vacuum at room temperature for 48 h.

Preparation of the PMMA–clay nanocomposite materials by solution dispersion

As a representative procedure, the PMMA–clay nanocomposite (PCN) materials were prepared by solution dispersion. First, the organophilic clay, the concentration of which was calculated to be 1, 3, or 5 wt % with respect to PMMA, was added to NMP under magnetic stirring for 24 h at room temperature. Commercial PMMA (M_w = 350,000) was subsequently added to the previous organophilic clay solution of NMP to form a 5 wt % PCN solution. Under magnetic stirring for an additional 12 h at room temperature, the as-prepared PCN solution was subsequently filtered with a 0.45-μm hydrophilic poly(vinylidene fluoride) filter (Millev-HV, Millpore) and cast onto a glass plate (5 cm $\times$ 5 cm, ~3 cc/pcs). This was followed by drying at approximately 50°C for 24 h to produce a PCN membrane.

Preparation of the coatings and electrochemical measurements

The uncoated CRS coupons were prepared before use with fine polishing paper, and this was followed by thorough washing with distilled water, acetone, and ethanol. The PMMA and PCN fine powders were then dissolved in NMP to produce typically 5 wt % solutions. The solutions were cast dropwise onto the coupons (1.0 cm $\times$ 1.0 cm), and this was followed by drying in air for 24 h at 50°C, which produced coatings approximately 35 μm thick, as measured with a digimatic micrometer (Mitutoyo). The coated and uncoated coupons were then mounted to the working electrode so that only the coated side of the coupon was in direct contact with the electrolyte. The edges of the coupons were sealed with a superfast epoxy cement. The electrochemical corrosion measurements were performed in a standard corrosion test cell equipped with two graphite rods (diameter = 6.15 mm) as counter electrodes, an SCE, and the aforementioned working electrode; a typical electrochemical cell is shown in Scheme 1. All the electrochemical measurements of E_{corr}, R_p, and i_{corr} were performed on a VoltaLab model 21 potentiostat/galvanostat and repeated at least three times. The electrolyte was an aqueous solution of NaCl (5 wt %). The open circuit potential (OCP) at the equilibrium state of the system was recorded as E_{corr} (vs SCE). R_p was measured by the sweeping of the applied potential from 20 mV below to 20 mV above E_{corr} at a scanning rate of 500 mV/min and by the recording of the corresponding current change. R_p was obtained from the slope of the potential–current plot. The Tafel plots were obtained by the scanning of the potential from 250 mV below to 250 mV above E_{corr} at a scanning rate of 500 mV/min. i_{corr} was determined through the superimposition of a straight line along the linear portion of the cathodic or anodic curve and its extrapolation through E_{corr}. The corrosion rate {R_{corr} [milli-inches per year (MPY)]} was calculated as follows:

$$R_{corr}\ (\mathrm{MPY}) = [0.13\ i_{corr}(\mathrm{EW})]/[Ad]$$

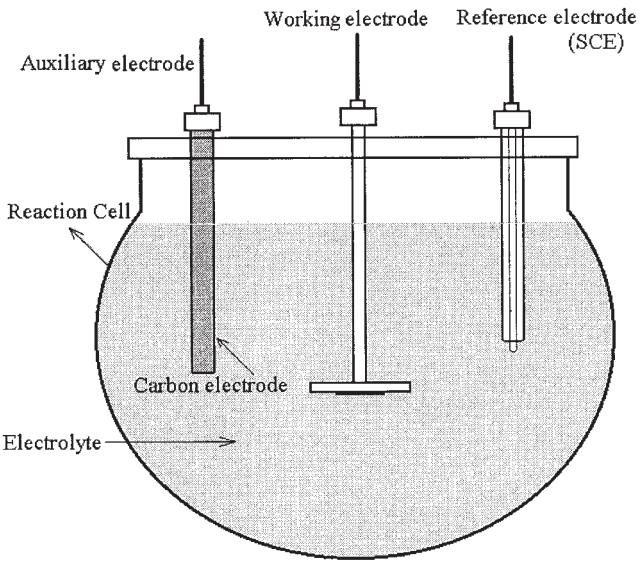

Scheme 1

where EW is the equivalent weight (g/equiv), A is the area (cm^2), and d is the density (g/cm^3).

A VoltaLab model 40 potentiostat/galvanostat was used to perform the impedance spectroscopy studies. Impedance measurements were carried out in the frequency range of 100 KHz to 100 MHz. First, the working electrode was kept in the test solution for at least 30 min so that it could reach an equilibrium state before the impedance run. This treatment put the electrode in a reproducible initial state and confirmed that no blistering occurred during the conditioning period. All the experiments were performed at room temperature (25± 1°C). All data were replicated at least three times to ensure reproducibility and statistical significance.

Preparation of the membrane and barrier property measurements

The membranes of as-synthesized PMMA or PCN materials were prepared for the measurement of the molecular (H_2O and O_2) barrier property. Typically, 0.1 g of as-synthesized PMMA or PCN materials was dissolved in 10 mL of NMP under magnetic stirring at room temperature for 4 h. The solution was cast onto a substrate (e.g., a microscope glass slide). The solvent was allowed to evaporate at 90–100°C under a hood for 24 h. The sample-coated glass substrate was then immersed into distilled water for 12 h to produce a membrane of PMMA and PCN materials, and this was followed by drying *in vacuo* for 24 h. The oxygen permeability of the membrane was determined with a Yanco GTR-10 gas permeability analyzer. Gas permeability P [cm^3(STP) cm/cm^2 s cmHg] was measured as follows:

$$P = l/(p1 - p2) \times \frac{q/t}{A}$$

where q/t is the volumetric flow rate of the gas permeate [cm^3(STP)/s]; l is the membrane thickness (cm); A is the effective membrane area (cm^2); and p_1 and p_2 are the pressures (cmHg) on the high-pressure and low-pressure sides of the membrane, respectively. The rate of transmission of O_2 was obtained by gas chromatography, and from this the air permeability was calculated. The water vapor permeation experiment was carried out with an apparatus used in our previously published studies.[8,9,13–17]

RESULTS AND DISCUSSIONS

PMMA can be polymerized by conventional free-radical polymerization through various polymerization techniques, such as bulk, solution, suspension, and emulsion processes. PMMA is used for many industrial applications (e.g., automotive parts, decorative paneling, skylights, and glazing). On the other hand, MMT is a clay mineral containing stacked silicate sheets approximately 1 nm thick and approximately 220 nm long.[23] The chemical structure of MMT consists of two fused silica tetrahedral sheets sandwiching an edge-shared octahedral sheet of either magnesium or aluminum hydroxide. In general, polymer–clay composites can be roughly divided into three main types—conventional composites (microcomposites), intercalated nanocomposites, and exfoliated nanocomposites—according to the different dispersion abilities of the clay platelets in the polymer framework. The three types of composites are shown in Figure 1.

In this study, the PMMA–clay nanocomposite (PCN) materials were prepared by *in situ* polymerization in two steps. First, the organophilic clay was prepared by a cation-exchange reaction between the sodium cations of the MMT clay and the alkylphosphonium ions of the intercalating agent. Such an organic modification provided two benefits: the interlayer region between the layered silicates increased because of the long-chain alkylphosphonium cations, thereby weakening the interaction between the successive clay layers, and small molecules electrostatically bonded to silicates led to MMT being more molecularly compatible with the polymer molecules. Second, organic MMA monomers were subsequently intercalated and diffused into the interlayer gallery of the organophilic clay hosts, and this was followed by typical *in situ* polymerization. The preparation of PCN materials by solution dispersion was also carried out via magnetic stirring to promote the uniform dispersion of the nanoclay platelets in the polymer framework. The compositions of the PCN materials pre-

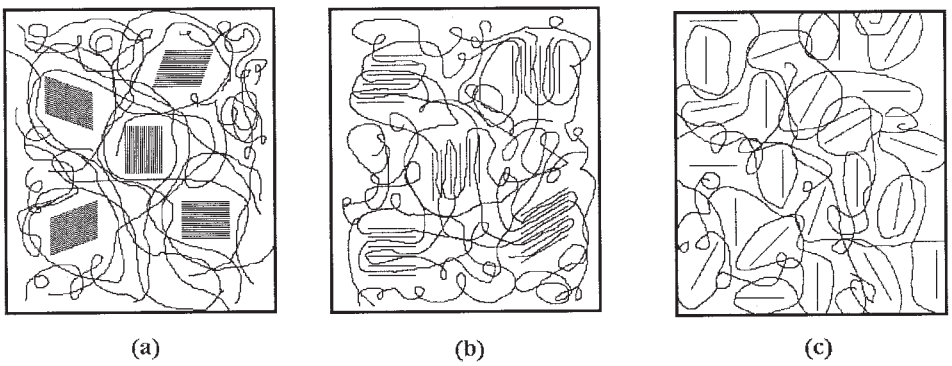

Figure 1 Three types of polymer–clay composites: (a) conventional composites (microcomposites), (b) intercalated nanocomposites, and (c) exfoliated nanocomposites.

pared with the two approaches varied from 0 to 5 wt % clay with respect to the PMMA content, as summarized in Table I.

Molecular weight determination of bulk PMMA and PMMA extracted from PMMA–clay nanocomposite materials prepared by *in situ* emulsion polymerization

The molecular weights (M_w) of the various as-prepared samples recovered from the interlayer regions of the MMT clay were obtained by gel permeation chromatography (GPC) analyses with THF used as the eluant. All the GPC elution patterns of the samples displayed a single peak, which corresponded to a specific molecular weight, as summarized in Table II. The M_w values of extracted PMMA obtained by *in situ* emulsion polymerization were significantly lower (e.g., M_w of ECMA3 = 351,100) than those of bulk PMMA (M_w of EPMMA = 519,300), indicating the structurally confined polymerization situations in the intragallery region of the MMT clay and the nature of the clay–oligomer interactions, such as adsorption, during the polymerization reaction.[7–9,13–17] As a control experiment, M_w of PMMA extracted from the PMMA–clay nanocomposite (PCN) materials prepared by solution dispersion was also investigated with GPC studies. However, M_w of PMMA extracted from PCN materials prepared by solution dispersion was found to closely approximate that of bulk PMMA.

For a reasonable comparative study of the physical properties of the PCN materials obtained with the two different approaches, ECMA3 and SCMA3 were chosen because they had very similar M_w values (351,100 vs 350,000) and the same clay loading (3 wt %). Therefore, property comparison studies were carried out, as

TABLE I
Relationship of the Composition of PMMA–Clay Nanocomposite Materials Prepared by Both *In Situ* Emulsion Polymerization and Solution Dispersion with the Thermal Stability, Gas Barrier, and Corrosion Protection Properties Measured by DSC, TGA, GPA, and Electrochemical Corrosion Measurements

	Feed Composition (wt %)		Thermal properties		Barrier properties[c]		Electrochemical corrosion measurements[d]			
Compound code	PMMA	MMT	T_g (°C)[a]	T_d (°C)[b]	O_2 (barrer)	H_2O (g/m^2 h)	E_{corr} (mv)	R_p ($10^3\Omega$ cm^2)	i_{corr} (nA/cm^2)	R_{corr} (MPY)
Bare	—	—	—	—	—	—	−628	36	2.7×10^3	5.2
EPMMA	100	0	98.7	281.6	0.811	177	−423	580	54	1.0×10^{-1}
ECMA1	99	1	103.2	287.3	0.631	136	−321	2700	27	5.2×10^{-2}
ECMA3	97	3	111.3	292.2	0.532	117	−219	3500	21	4.1×10^{-2}
ECMA5	95	5	120.7	296.5	0.442	104	−203	6100	11	2.1×10^{-2}
SPMMA	100	0	97.7	277.3	0.951	236	−546	240	76	1.5×10^{-1}
SCMA1	99	1	101.7	280.6	0.933	206	−431	250	60	1.2×10^{-1}
SCMA3	97	3	103.2	282.7	0.777	204	−369	370	56	1.1×10^{-1}
SCMA5	95	5	113.6	285.1	0.726	191	−330	2100	33	6.3×10^{-2}

[a] As measured by DSC.
[b] As measured by TGA.
[c] As determined by GPA.
[d] An SCE was employed as the reference electrode.

TABLE II
Molecular Weight and Molecular Weight Distribution of PMMA Extracted from PCN Materials Prepared by *In Situ* Emulsion Polymerization

Sample code	M_w	M_n	M_w/M_n
EPMMA	519,300	235,000	2.20
ECMA1	460,500	213,000	2.16
ECMA3	351,100	170,000	2.12
ECMA5	277,000	133,000	2.08

M_n = number-average molecular weight.

detailed in the following sections, mainly on the basis of these two samples.

Optical clarity of the PMMA–clay nanocomposite membranes

The optical clarity of the PCN materials in membrane form prepared by the two approaches can be compared via UV–vis transmission spectroscopy studies. First, we found that the optical clarity of both neat polymer membranes (i.e., EPMMA and SPMMA) showed approximately high transparency, as shown in Figure 2. However, the UV–vis transmission spectrum of ECMA3 showed much higher transparency than that of SCMA3. The obvious difference in the optical clarity of the PCN membranes (i.e., ECMA3 and SCMA3) could be associated with the different dispersion degrees and abilities of the nanoclay layers in the polymer framework. Generally, the optical clarity of PCN materials with a better dispersion of clay platelets showed higher transparency than that of materials with a poor dispersion of clay nanolayers in the polymer matrix. Therefore, we believe that ECMA3 had a better dispersion of clay platelets than SCMA3. These results were further reconfirmed by the following powder XRD pattern studies and TEM observations.

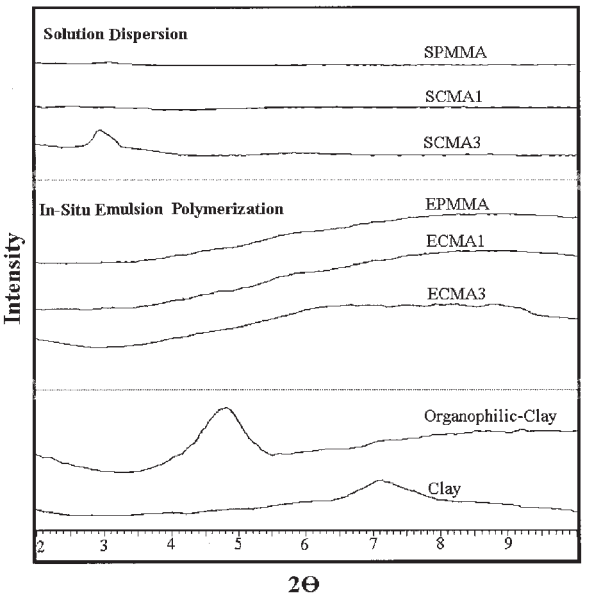

Figure 3 Wide-angle powder XRD patterns of clay, organophilic clay, PMMA, and PMMA–clay nanocomposites prepared by both *in situ* polymerization and solution dispersion.

Powder XRD patterns and TEM

Figure 3 shows wide-angle powder XRD patterns of the organophilic clay and a series of PCN materials

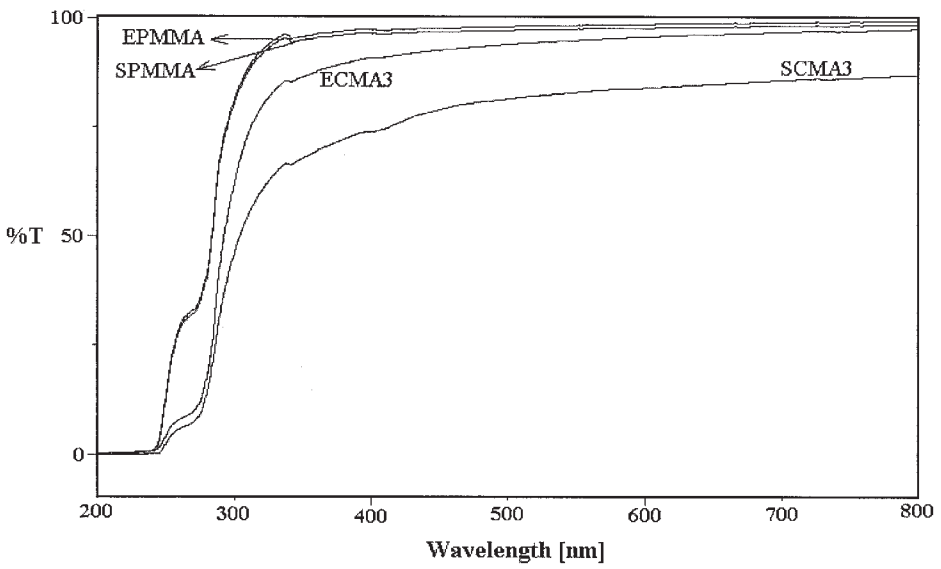

Figure 2 UV–vis transmission spectra of PMMA and PMMA–clay nanocomposite membranes: EPMMA, SPMMA, SCMA3 (intercalated structures), and ECMA3 (exfoliated structures).

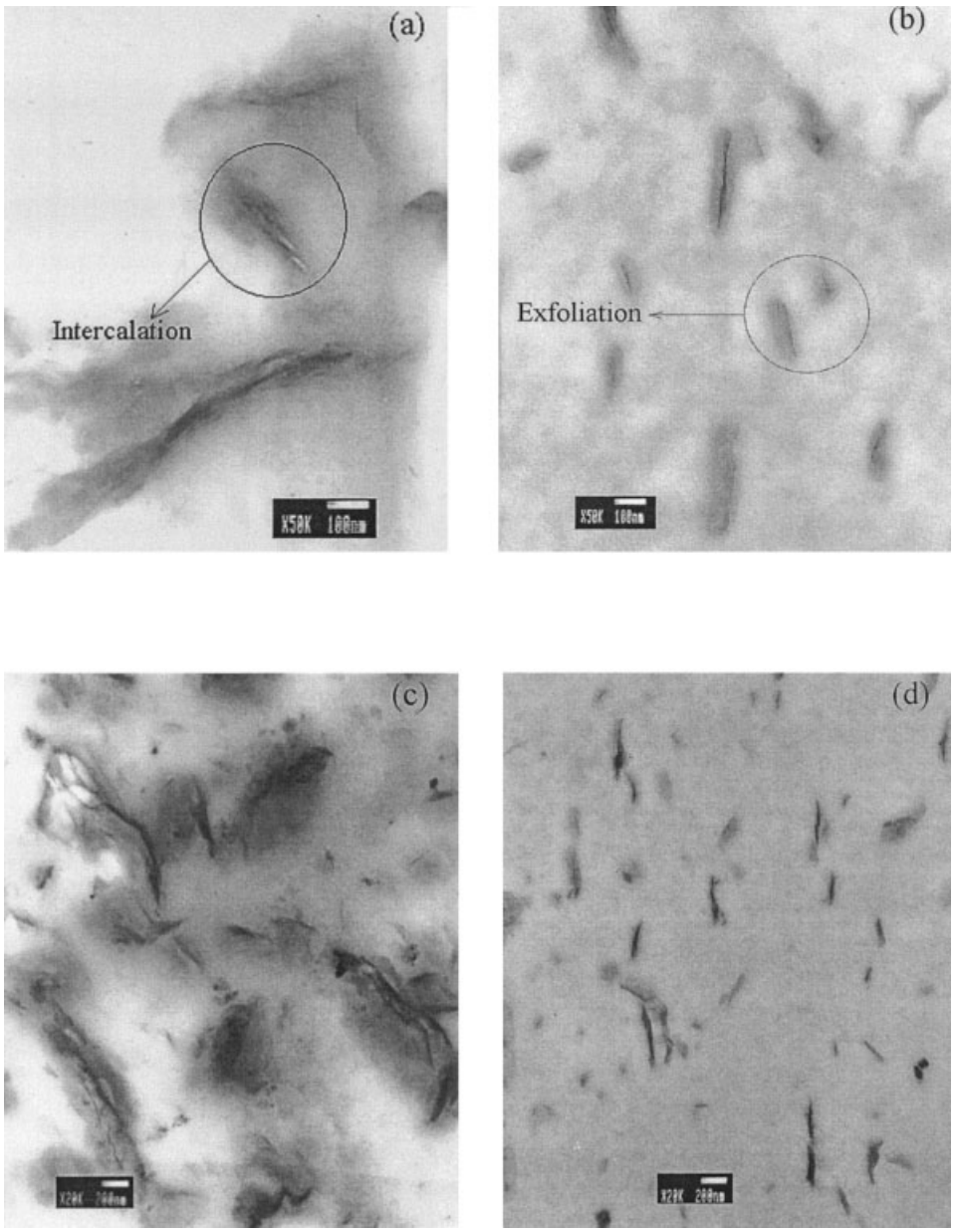

Figure 4 TEM micrographs of (a) SCMA3 at 50,000×, (b) ECMA3 at 50,000×, (c) SCMA3 at 20,000×, and (d) ECMA3 at 20,000×.

obtained with both approaches. In the *in situ* emulsion polymerization approach to preparation of PMMA–clay nanocomposites with up to 3 wt % clay (i.e., ECMA3), there was no diffraction peak at 2θ = 2–10°, but there was a diffraction peak at 2θ = 4.70° (*d*-spacing = 1.86 nm) for the organophilic clay; this indicated the probability of exfoliated silicate nanolayers of the organophilic clay dispersed in the PMMA matrix. However, with solution dispersion, when the loading of the organoclay increased up to 3 wt % (i.e., SCMA3), a peak appeared at 2θ = 2.92°, corresponding to a *d*-spacing of 3.03 nm. This implied that there was a small amount of the organoclay that could not be exfoliated in PMMA and existed in the form of an intercalated layer structure. In conclusion, ECMA3 exhibited better dispersion (mainly an exfoliated or intercalated morphology with larger *d*-spacing) and SCMA3 showed poor dispersion of the clay nanolayers (an intercalated morphology with small *d*-spacing) in the polymer matrix according to the powder XRD studies. In Figure 4, the TEM micrograph of ECMA3 does reveal a better dispersion of clay nanolayers in the PMMA matrix than that of SCMA3. For example, for ECMA3, individual silicate layers, along with two- and three-layer stacks, showed better dispersion in the PMMA matrix at magnifications of 50,000 and 20,000×, as shown in Figure 4(b,d). However, for SCMA3, the majority of the area that appeared con-

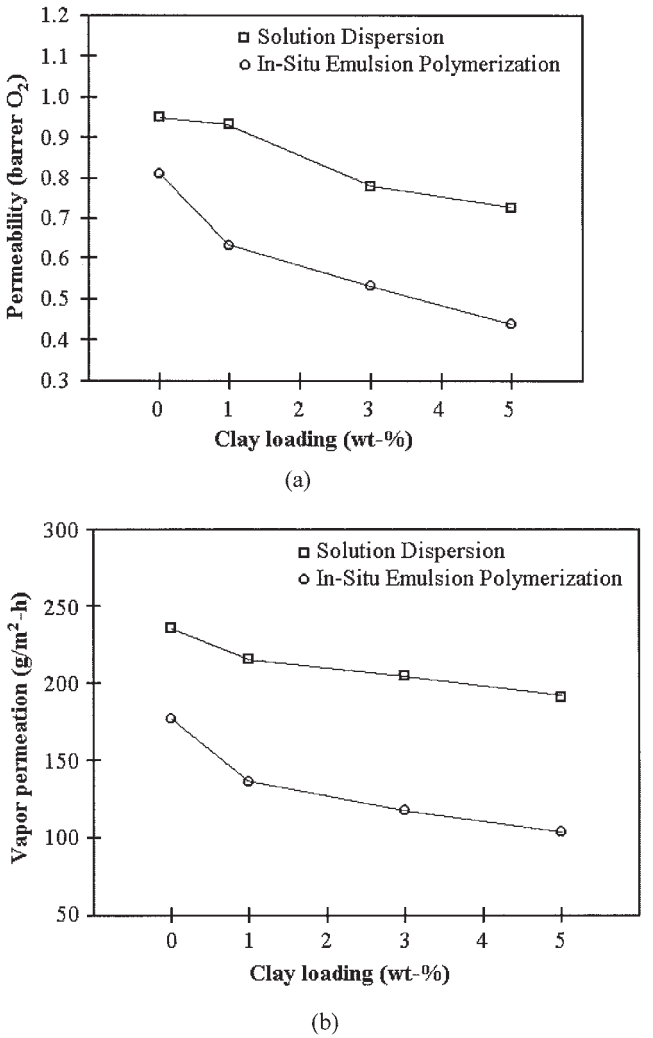

Figure 5 Permeability of (a) O_2 and (b) water vapor as a function of the MMT clay content in the PMMA–clay membranes prepared by both approaches.

sisted of larger intercalated tactoids (i.e., poor dispersion), as shown in Figure 4(a,c). The morphology observations based on the TEM studies were consistent with those of previous powder XRD pattern studies.

Molecular barrier of the membranes

The membranes of PCN materials and neat PMMA used for the molecular barrier measurements were prepared to have a film thickness of approximately 70 μm. In comparison with neat PMMA, the PCN membranes prepared by both approaches exhibited lower O_2 and water vapor permeability, as shown in Figure 5(a,b) and Table I. In addition, the O_2 and water vapor permeability of ECMA3 (0.532 barrer and 117 g/m^2 h) was significantly lower than that of SCMA3 (0.777 barrer and 204 g/m^2 h). This enhanced gas/vapor barrier effect of ECMA3, with respect to that of SCMA3, could be associated with ECMA3 having a better dispersion of clay platelets in the PMMA matrix, which led to a longer tortuosity of the diffusion pathway of oxygen and water, as shown in Scheme 2. Furthermore, a further increase in the clay loading resulted in a slightly more enhanced molecular barrier property of bulk PCN materials with both approaches.

Corrosion protection performance of the coatings

We have demonstrated that the dispersion of nanoclay platelets in a polymer framework can effectively enhance the gas/vapor barrier property of the neat polymer in the form of a film because of the increase in the tortuosity of the pathways of oxygen and water, leading to potential industrial applications as enhanced corrosion protection coatings.[8,9,13–17] Basically, electrochemical methods (e.g., E_{corr}, R_p, i_{corr}, and impedance spectroscopy) were used to speed up the evaluation of the anticorrosion performance of as-prepared materials on CRS coupons, as listed in Table I. OCP at the equilibrium state of the system was recorded as E_{corr} (vs SCE). After 30 min of corrosion testing, the CRS coupon coated with PMMA showed a higher E_{corr} value than the uncoated CRS. Furthermore, PMMA with a higher M_w value (i.e., for EPMMA, 519,300) had a higher E_{corr} value than that with a lower M_w value (i.e., for SPMMA, 350,000). However, it had a lower E_{corr} value than the specimen coated with PCN materials, and this shows that the dispersion of nanoclay platelets into a polymer framework may enhance the corrosion protection effect of a neat polymer on a metallic surface.[8,9,13–17] For example, the ECMA3-coated CRS had a high E_{corr} value of about -219 mV at 30 min. Even after 5 h of measurement, the potential remained at about -225 mV. Such an E_{corr} value implies that the ECMA3-coated CRS had enhanced corrosion protection toward electrochemical corrosion in comparison with SCMA3 ($E_{corr} = -369$ mV). Furthermore, the ECMA3-coated CRS also showed an R_p value of 3.5×10^6 Ω cm^2 in 5 wt % NaCl, about one order of magnitude greater than that of the SCMA3-coated CRS ($R_p = 3.7 \times 10^5$ Ω cm^2; Table I). Tafel plots for uncoated, SPMMA-coated, SCMA3-coated, and ECMA3-coated CRS are shown in Figure 6. For example, i_{corr} of ECMA3-coated CRS was about 21 nA/cm^2, which corresponded to an R_{corr} value of about 4.1×10^{-2} MPY (Table I). However, i_{corr} of SCMA3-coated CRS was about 56 nA/cm^2 ($R_{corr} = 1.1 \times 10^{-1}$ MPY). In summary, a PCN coating with better dispersion (e.g., ECMA3) provided better corrosion protection than that with poor dispersion (e.g., SCMA3) according to the electrochemical corrosion measurements of E_{corr}, R_p, and i_{corr}.

Recently, electrochemical impedance spectroscopy (EIS) was used to study the activity difference between CRS surfaces after PMMA and PCN treatments.[9,14,15] In this study, four samples were pre-

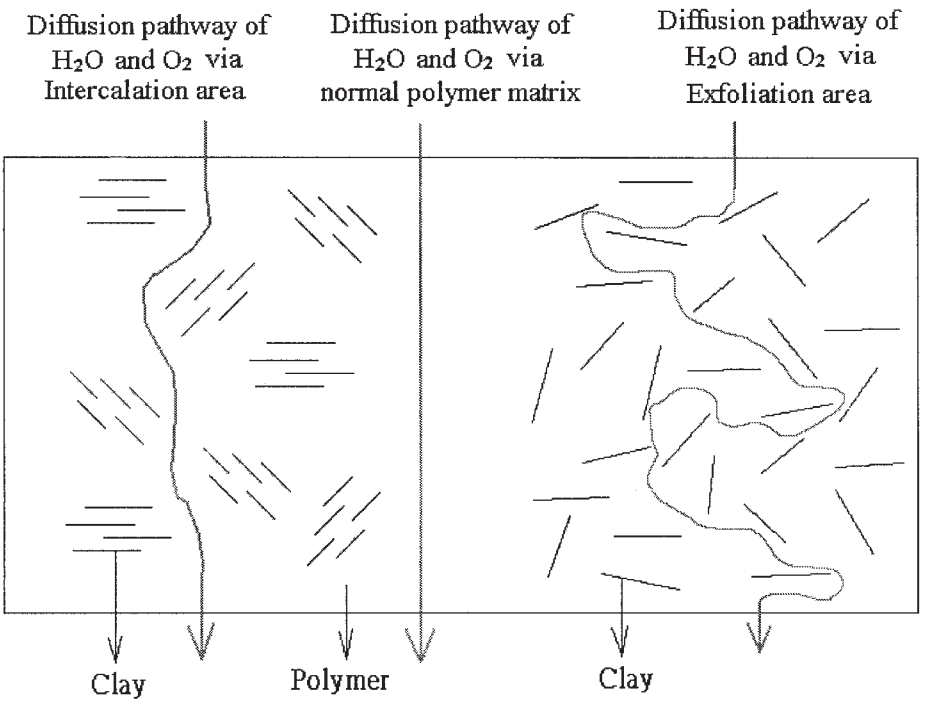

Scheme 2

pared. The first sample was uncoated CRS. Samples labeled SPMMA, SCMA3, and ECMA3 were CRS-coated with various as-prepared materials. The electrochemical corrosion testing of these samples in 5 wt % NaCl aqueous electrolytes for 30 min was followed by EIS. Figure 7 shows the Nyquist plots of the four samples. The charge-transfer resistances of the samples, as determined by the intersection of the low-frequency end of the semicircle arc with the real axis, were 11.5, 252.7, 472.5, and 3098.9 kΩ cm^2, respectively. The results clearly demonstrate that the sample prepared by *in situ* polymerization with a better dispersion of clay platelets provided better anticorrosive performance, and this was consistent with the conclusions obtained from previous electrochemical measurements.

Thermal properties of the fine powders

Figure 8 shows the relationship between the thermal decomposition temperature (T_d) of PCN materials and

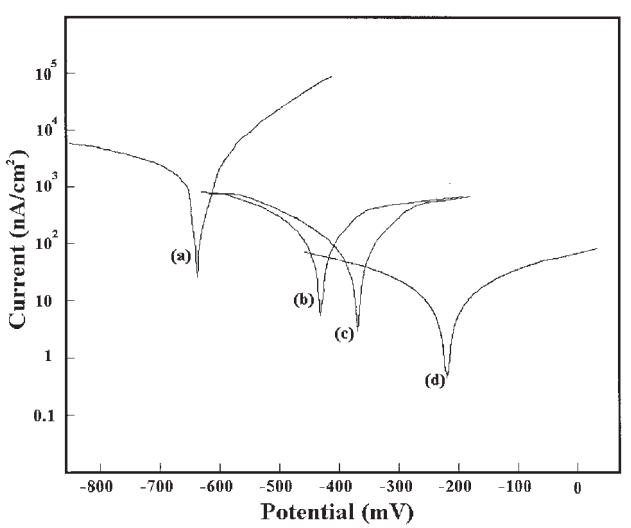

Figure 6 Tafel Plots for (a) uncoated, (b) SPMMA, (c) SCMA3, and (d) ECMA3-coated CRS measured in 5 wt % NaCl aqueous solutions.

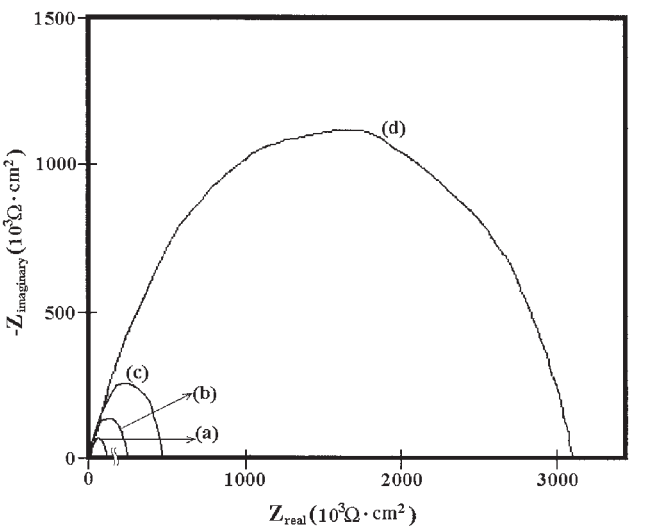

Figure 7 Nyquist plots of four CRS samples in 5 wt % NaCl aqueous solutions: (a) uncoated, (b) SPMMA, (c) SCMA3, and (d) ECMA3.

the weight percentage (wt %) of the clay loading, as obtained from TGA measurements in an air atmosphere on membranes of PMMA and PCN materials prepared with both approaches. Evidently, T_d of the PCN materials prepared with both approaches shifted toward a higher temperature range than that of neat PMMA, and this confirmed the enhancement of the thermal stability of the intercalated and exfoliated composites. However, the exfoliated composite (e.g., ECMA3) exhibited higher thermal stability enhancement than the intercalated composite (e.g., SCMA3) with the same clay loading. For example, ECMA3 displayed an approximately 10°C increase in T_d over that of SCMA3, as shown in Table I, and this showed that PCN with exfoliated structures had better thermal stability enhancement than that with intercalated structures with the same clay loading on the basis of TGA studies. Furthermore, DSC traces of the neat PMMA and PCN materials are shown in Figure 9. The neat EPMMA exhibited a baseline shift at 98.7°C corresponding to the glass-transition temperature (T_g) of PMMA. T_g of the composites increased with an increasing concentration of clay platelets in the polymer framework, as shown in Table I. This was tentatively attributed to the confinement of the intercalated polymer chains within the clay galleries, which prevented the segmental motions of the polymer chains. The composites prepared by *in situ* polymerization exhibited higher T_g's than their counterparts. For example, ECMA3 (T_g = 111.3°C) showed an obvious increase in T_g over that of SCMA3 (103.2°C). This phenomenon can be explained as follows: the composite showing an exfoliated or intercalated structure with larger *d*-spacing that resulted from *in situ* polymerization significantly enhanced the interfacial interactions (in comparison with the intercalated composite) between the organic polymer framework and the inorganic clay platelets, and this led to an increasingly restricting strength of the clay nanolayers on the PMMA molecules.

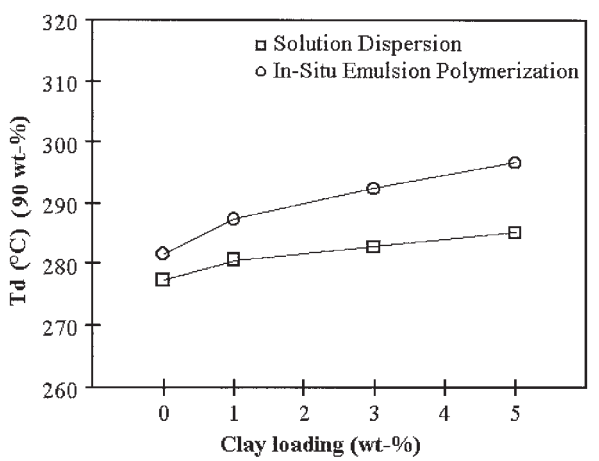

Figure 8 T_d of PCN materials as a function of the clay content in the PMMA–clay nanocomposites prepared by both approaches.

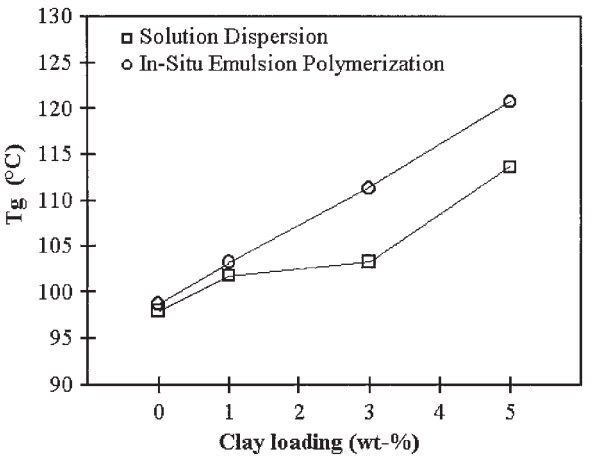

Figure 9 T_g of PCN materials as a function of the clay content in the PMMA–clay nanocomposites prepared by both approaches.

CONCLUSIONS

A series of PCN materials were prepared through the effective dispersion of the inorganic nanolayers of MMT clay in an organic PMMA matrix via both *in situ* polymerization and solution dispersion. The as-synthesized PCN material prepared by *in situ* polymerization (e.g., ECMA3) showed better dispersion of the clay platelets than that prepared by solution dispersion (e.g., SCMA3) according to powder XRD and TEM studies. ECMA3 coated on CRS was far superior in anticorrosion properties than SCMA3 according to a series of electrochemical measurements in 5 wt % aqueous NaCl electrolytes. The enhanced anticorrosion of ECMA3 on CRS in comparison with bulk SCMA3 in the form of a coating might have resulted from the better dispersion of the silicate nanolayers of clay in the PMMA framework, which further increased the tortuosity of the diffusion pathways of oxygen and water. ECMA3 also exhibited better barrier properties, optical clarity, and thermal stability than SCMA3 according to GPA, UV–vis transmission spectroscopy, TGA, and DSC.

References

1. Giannelis, E. P. Adv Mater 1996, 8, 29.
2. Novak, B. M. Adv Mater 1993, 5, 422.
3. Komarneni, S. J Mater Chem 1992, 2, 1219.
4. Usuki, A.; Kojima, Y.; Kawasumi, M.; Okada, A.; Kukushima, Y.; Kurauchi, T.; Kamigaito, O. J Mater Res 1993, 8, 1179.
5. Yano, K.; Usuki, A.; Kurauchi, T.; Kamigaito, O. J Polym Sci Part A: Polym Chem 1993, 31, 2493.
6. Massersmith, P. B.; Giannelis, E. P. Chem Mater 1994, 6, 1719.

7. Yeh, J.-M.; Liou, S.-J.; Chang, Y.-W. J Appl Polym Sci 2004, 91, 3489.
8. Yu, Y.-H.; Yeh, J.-M.; Liou, S.-J.; Chang, Y.-P. Acta Mater 2004, 52, 475.
9. Yu, Y.-H.; Jen, C.-C.; Huang, H.-Y.; Wu, P.-C.; Huang, C.-C.; Yeh, J.-M. J Appl Polym Sci 2004, 91, 3438.
10. Messersmith, P. B.; Giannelis, E. P. J Polym Sci Part A: Polym Chem 1995, 33, 1047.
11. Burnside, S. D.; Giannelis, E. P. Chem Mater 1995, 7, 1597.
12. Vaia, R. A.; Vasudevan, S.; Krawiec, W.; Scanlon, L. G.; Giannelis, E. P. Adv Mater 1995, 7, 154.
13. Yeh, J.-M.; Liou, S.-J.; Lai, C.-Y.; Wu, P.-C.; Tsai, C.-Y. Chem Mater 2001, 13, 1131.
14. Yeh, J.-M.; Liou, S.-J.; Lin, C.-Y.; Cheng, C.-Y.; Chang, Y.-W.; Lee, K.-R. Chem Mater 2002, 14, 154.
15. Yeh, J.-M.; Chen, C.-L.; Chen, Y.-C.; Ma, C.-Y.; Lee, K.-R.; Wei, Y.; Li, S. Polymer 2002, 43, 2729.
16. Yeh, J.-M.; Chin, C.-P. J Appl Polym Sci 2003, 88, 1072.
17. Yeh, J.-M.; Chin, C.-P.; Chang, S. J Appl Polym Sci 2003, 88, 3264.
18. Usuki, A.; Kawasumi, M.; Kojima, Y.; Okada, A.; Karauchi, T.; Kamigaito, O. J Mater Res 1993, 8, 1774.
19. Huang, X.; Lewis, S.; Brittain, W.-J.; Vaia, R. A. Macromolecules 2000, 33, 2000.
20. Chen, G.; Chen, X.; Lin, Z.; Ye, W.; Yao, K. J Mater Sci Lett 1999, 18, 1761.
21. Okamoto, M.; Morita, S.; Taguchi, H.; Kim, Y. H.; Kotaka, T.; Tateyama, H. Polymer 2000, 41, 3887.
22. Biasci, L.; Aglietto, M.; Ruggeri, G.; Ciardelli, F. Polymer 1994, 35, 3296.
23. Bhattacharya, J.; Chakraborti, S. K.; Talapatra, S. J Polym Sci Part A: Polym Chem 1989, 27, 3977.
24. Lee, D. C.; Jang, L. W. J Appl Polym Sci 1996, 61, 1117.
25. Munzer, M.; Trommsdorff, E. In Polymerization Process; Schildknecht, C. E.; Skeist, I., Eds.; Wiley: New York, 1977.
26. Yano, K.; Usuki, A.; Okada, A. J Polym Sci Part A: Polym Chem 1997, 35, 2289.
27. Huang, X.; Brittain, W. J. Macromolecules 2001, 34, 3255.
28. Chern, C.-S.; Lin, C. H. Polymer 2000, 41, 4473.